NASA TECHNICAL MEMORANDUM

NASA TM X-936

15 p.

ENERGY ABSORBER FOR THE ARIEL I INSTRUMENT BOOMS

by T. L. Eng

NASA
Goddard Space Flight Center
Greenbelt, Maryland

NATIONAL AERONAUTICS AND SPACE ADMINISTRATION • WASHINGTON, D. C. • JANUARY 1964

ENERGY ABSORBER FOR THE ARIEL I INSTRUMENT BOOMS

T. L. Eng
Goddard Space Flight Center

NATIONAL AERONAUTICS AND SPACE ADMINISTRATION

ENERGY ABSORBER FOR THE ARIEL I INSTRUMENT BOOMS

by
T. L. Eng
Goddard Space Flight Center

SUMMARY 12873

The instrument boom energy absorber aboard the Ariel I was designed on the principle of runaway escapement. Its function was to reduce the erection rate of the instrument booms, thereby minimizing the kinetic energy transferred to these booms during their deployment and thus further safeguarding the experiments carried by the booms from shock damages. This device consisted of a pulley coupled to a gear train, which in turn was regulated by a pallet on a scape wheel. Since the frequency of the pallet is a function of the actuating torque, its amplitude, and moment of inertia, the rate of movement of the escapement mechanism can be adjusted by making the pallet moment of inertia variable (the others constant).

Ariel I was successfully launched on April 26, 1962. Telemetry data from the satellite indicated that all experiments carried by the booms had functioned normally.

AUTHOR

CONTENTS

ENERGY ABSORBER FOR THE ARIEL I INSTRUMENT BOOMS

by
T. L. Eng
Goddard Space Flight Center

INTRODUCTION

The first successfully launched satellite of the International Space Exploration program, Ariel I (1962) had two booms—each carrying a scientific experiment (the electron density and the electron temperature sensors) on its outer end. These booms were placed along the side of the last stage during flight and were released at a predetermined time and allowed to deploy by centrifugal force. Calculations indicated that, for the spacecraft to achieve the desired final spin rate, these booms must be released at the time when the satellite is spinning at 74 rpm. Further calculations showed that approximately 0.3 second would be required for the unrestrained booms to be fully deployed. At the instant when these booms cease traveling and are locked in their final position, they would be required to absorb 33 ft-lb of energy. Therefore to safeguard the above-mentioned experiments and ultimately protect the useful life of the satellite, the energy transferred to the booms during their deployment should be reduced.

DESIGN CONSIDERATIONS AND ANALYSIS

Requirements

The selected design, which would reduce the energy transferred to the booms, must also be:

1. A self-actuating device containing no out-gassing materials which might contaminate the experiments;

2. Capable of controlling the booms simultaneously so that they may erect together or within a fraction of a second of each other;

3. Capable of varying the erection time to not less than 1 second at the anticipated boom release spin rate and capable of withstanding a load equivalent to a 20 percent overspin or 90 rpm;

4. Light and capable of being housed in existing available space; and

5. Able to meet the environmental test specifications at the prototype level.

The second condition indicated that the mechanism should be centrally located. The only available room in the central area was the space (7 in. diam. × 2 in.) below the tape recorder, where the middl portion was occupied by an electron temperature gauge (Figure 1).

To satisfy all conditions, a constant velocity device—an escapement mechanism (similar to th clock mechanism)—was selected (Figure 2). Since the kinetic energy of a moving mass is proportion to its velocity square, $KE = 1/2\,MV^2$, theoretically, by controlling the erection rate or V of the boom the energy transferred to them is also controlled.

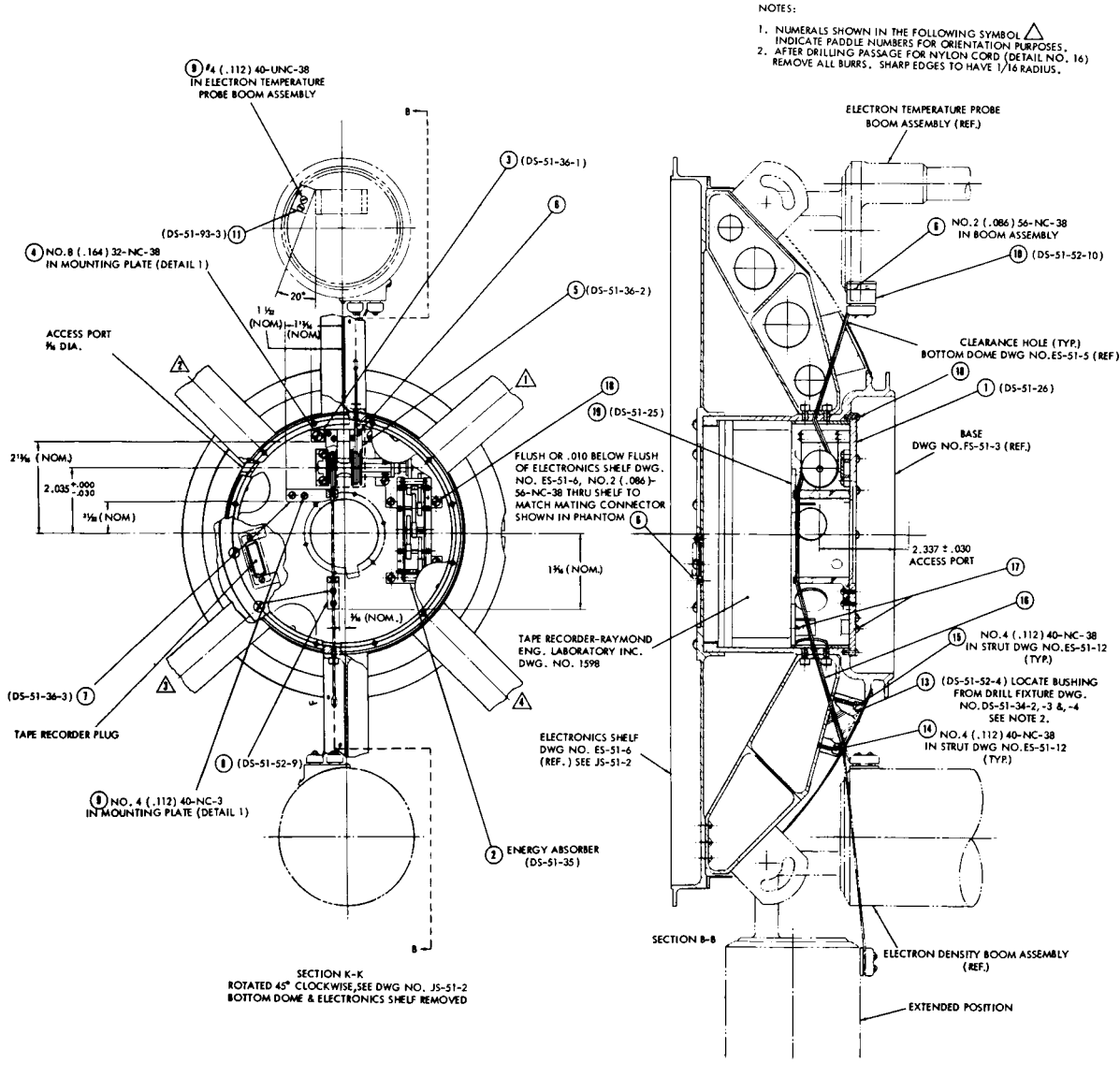

Figure 1—Location of Energy Absorber in Relation to the Instrument Boom.

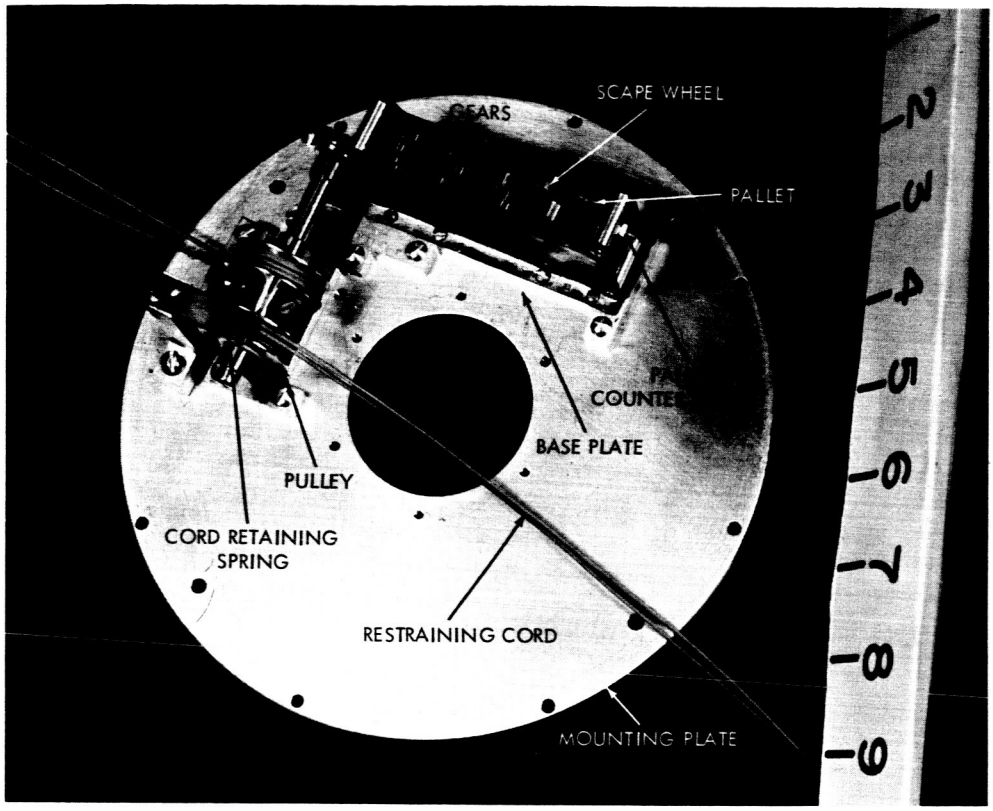

Figure 2—The Escapement Mechanism.

Force Analysis

To simplify the force analysis on the booms, frictional forces at the hinge were neglected. It was also assumed that at the time of boom deployment the satellite was in an environment of weightlessness; consequently, the weight of the boom assembly was not considered. The force with which the energy absorber is directly concerned is the centrifugal force acting on the booms, and it was further assumed that this force acted through the center of mass of the boom assembly (see Reference 1 and Figure 3):

$$F_{m+M} = M' \bar{r} \phi^2 \ , \tag{1}$$

where $M' = m + M$, m is the mass of concentrated weight, M the mass of the boom, $\bar{r}$ the distance to the boom's cg from the spin axis, F_{m+M} the centrifugal force acting on the center of mass, and ϕ the spin rate of the satellite at any given θ, the boom position at any given time. If

$$\bar{r} = a + \bar{L} \sin \theta \ , \tag{2}$$

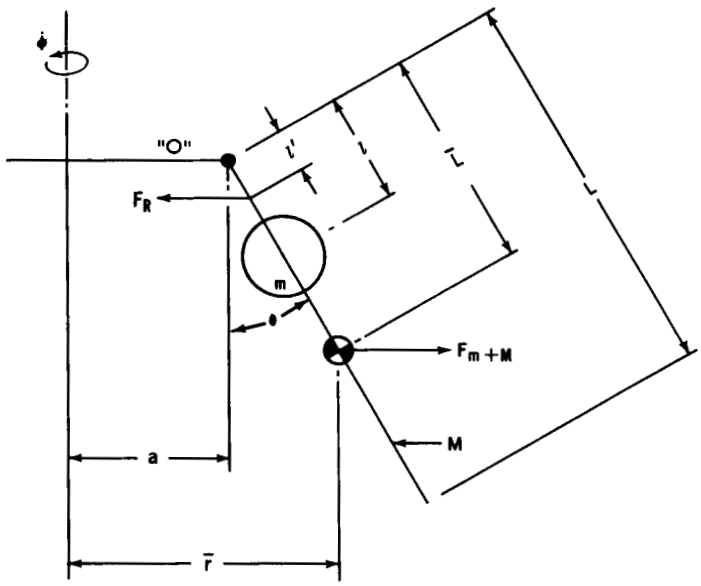

Figure 3—"Free Body" Schematic of Satellite.

we have

$$F_{m+M} = M' \dot{\phi}^2 (a + \bar{L} \sin\theta) , \tag{3}$$

where $\bar{L}$ is the distance from the pivot end of the boom to the center of mass M', and a the distance from the spin axis to the boom hinge. The sum of the moments about the pivot point is zero:

$$\Sigma M_0 = 0 ;$$

therefore the reaction force

$$F_R = \frac{F_{m+M} \bar{L} \cos\theta}{l' \cos\theta} \tag{4}$$

where l' is the location of the restraining point of the energy absorber. Thus, for $\theta < 90°$, we have

$$F_R = \frac{F_{m+M} \bar{L}}{l'} \tag{5}$$

and by substituting Equation 3 into 5, we obtain

$$F_R = \frac{M' \dot{\phi}^2 (a + \bar{L} \sin\theta) \bar{L}}{l'} , \tag{6}$$

where F_R is the restraining force from the escapement mechanism required to set one boom at equilibrium at any given position, θ. Since there were two booms, the total force acting on the energy absorber would be 2 F_R. To evaluate $\dot{\phi}$ in terms of θ at any given $\dot{\phi}_0$, the satellite's spin rate prior to deployment, the following equation was used:*

$$\frac{\dot{\phi}}{\dot{\phi}_0} = \frac{(m+M)a^2 + I}{m(l \sin\theta + a)^2 + M\left(\frac{\bar{L}}{3} \sin^2\theta + aL \sin\theta + a^2\right) + I} , \tag{7}$$

where Figure 4 shows that F_{m+M} maximized at approximately 35°; therefore the design load for the energy absorber would be $F_{m+M} \bar{L}/l'$ at $\theta = 35°$. I is the moment of inertia of the satellite prior to appendage deployment.

*J. V. Fedor, Private communication.

The actuating force, F_A, on the escapement mechanism (per boom) is as shown in Figure 5.

$$F_A = \frac{l'}{L} F_{m+M} \qquad (8)$$

To insure the actuation of the energy absorber under most conditions, a minimum F_A was chosen. In this case, where F_A does practically no work when $\theta \geq 60°$, it was assumed that F_A is minimum when $\theta = 60°$.

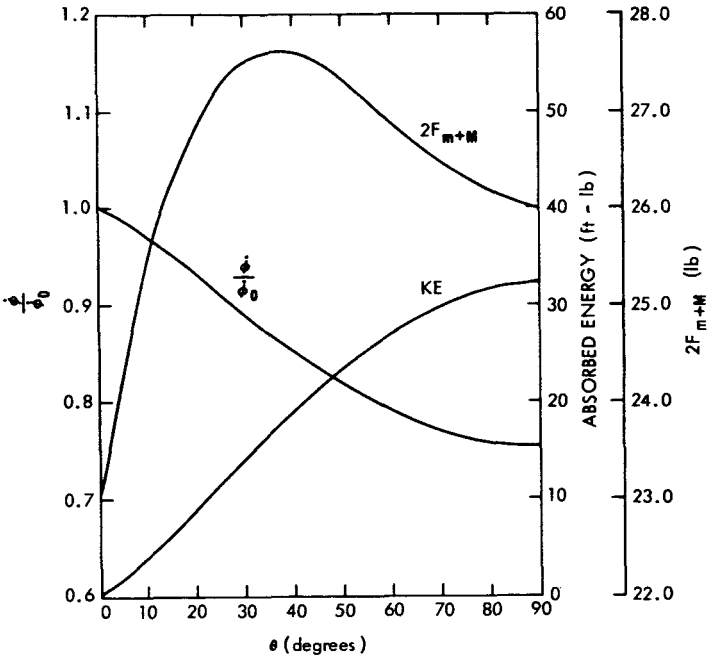

Figure 4—Calculated Results based on ϕ_0 = rpm.

Escapement Design

The expression for a pallet half-cycle period for a runaway escapement (References 2 and 3) is

$$t_1 = \sqrt{\frac{2I_{p_1}\theta_1}{T_{p_1}}}, \qquad (9)$$

where θ_1 denotes the half-cycle amplitude, I_{p_1} the moment of inertia of one half the pallet, and T_{p_1} the torque acting on the pallet. Total pallet amplitude θ is $\theta_1 + \theta_2 = 2\pi/n$, where n is the number of teeth on the scape wheel. For cases where the first and second half-cycle motions are identical, the pallet frequency f is equal to 1/t or

$$f = \frac{1}{2}\sqrt{\frac{T_{p_1}}{2I_{p_1}\theta_1}}. \qquad (10)$$

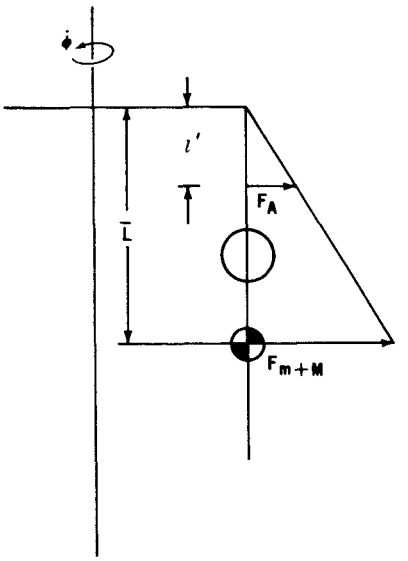

Figure 5—Forces acting on the Energy Absorber.

The first half-cycle period for the scape wheel is

$$t_1 = \sqrt{\frac{2I_{e_1}\theta_1}{T_w}}, \qquad (11)$$

where $T_w/T_p = \omega_p/\omega_n$ and the equivalent moment of inertia $I_e = I_w + I_p\left(\omega_p/\omega_w\right)^2$ and T_w is the torque acting on the scape wheel, I and ω the mass moment of inertia and angular velocity respectively.

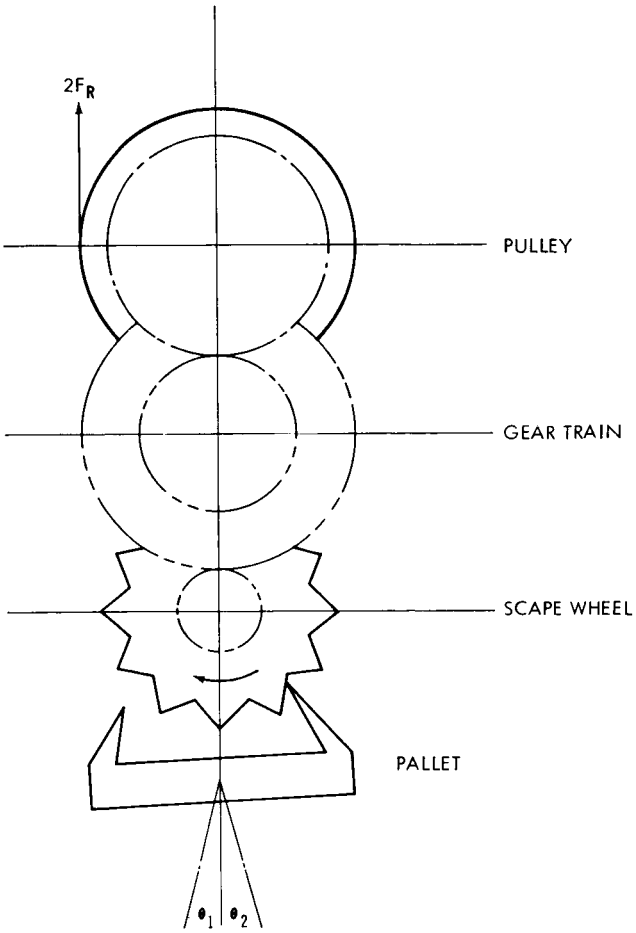

Figure 6—Schematic of escapement design.

Subscripts p and w refer to the pallet and scape wheel. A similar expression is obtained for the second half of the pallet cycle:

$$t_1 + t_2 = \frac{1}{f} = \sqrt{\frac{2I_{e_1}\theta_1}{T_w}} + \sqrt{\frac{2I_{e_2}\theta_2}{T_w}}. \qquad (12)$$

In this instance, accuracy in timing was not an essential factor; thus we can simplify calculations by assuming that the motion of the first and second half pallet cycle were the same: $\theta_1 = \theta_2$, $t_1 = t_2$, $T_{p_1} = T_{p_2}$ $I_{p_1} = I_{p_2}$, and $I_{e_1} = I_{e_2}$.

Equations 9, 10, 11 and 12 now become:

$$t_1 = t_2 = \sqrt{\frac{I_p\theta}{T_p}}, \qquad (13)$$

$$f = \frac{1}{2}\sqrt{\frac{T_p}{I_p\theta}}, \qquad (14)$$

$$t_1 = t_2 = \sqrt{\frac{I_e\theta}{2T_w}}, \qquad (15)$$

$$t_1 + t_2 = \frac{1}{f} = \sqrt{\frac{I_e\theta}{T_w}}, \qquad (16)$$

respectively. To compensate for the inaccuracy of the mechanism owing to the simplified assumptions made in the calculations and to provide for a timing adjustment, I_p was made variable by attaching a counter weight to the pallet (Figure 2). By assuming that the actuating torque is constant and by varying the counter weight which changes I_p, t can be increased or decreased with the I_p changes indicated in the previous equations. The evaluation of T_w and T_p was based on F_a (Equation 8, where θ = 60°).

Gear Train Design

In calculating the stresses for the gears and shafts, the following assumptions were made:

1. The shaft between gears was in torsion;

2. The bearing portions of the shaft were in bending;

3. The pallet shaft was in bending.

The size of the shafts were evaluated by the following equations based on the maximum load determined by Equation 6 (Reference 4):

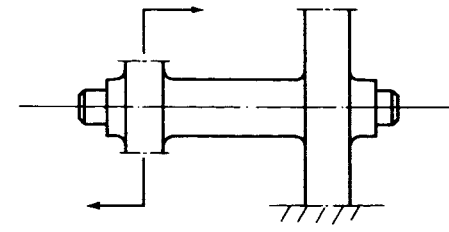

Figure 7—Schematic of the shafts.

$$\text{For shear under bending, } D^3 = \frac{16}{S_s \pi} M_b ; \qquad (17)$$

$$\text{For shear under torsion, } D^3 = \frac{16}{S_s \pi} M_t ; \qquad (18)$$

$$\text{For tensile under bending, } D^3 = \frac{32}{S_t \pi} M_b ; \qquad (19)$$

$$\text{For tensile under torsion, } D^3 = \frac{32}{S_t \pi} M_t ; \qquad (20)$$

where S_s is the shearing stress, S_t the tensile stress, M_b the bending moment, M_t the torsion moment, and D the shaft diameter. From these calculations, the larger value of D was accepted as the final dimension. The design load for the gear train was the same as the shaft design load. Since there were two booms, the total load on the first gear and shaft would be $2F_R$. The load on each succeeding gear and shaft decreased by a factor of $1/R$, where R is the gear ratio. Gear size was governed by the Lewis formula:

$$S = \frac{2M_t P_d}{K\pi^2 yN} \qquad (21)$$

where M_t is the torsion moment, P_d the diametrical pitch, y the form factor, N the number of teeth, and $K = P_d b/\pi$. In Equation 21, the allowable stress $S = S_0\ (1200/(1200 + V))$, where S_0 is the ultimate strength and V the pitch-line velocity. The selected gear size must also satisfy the dynamic tooth load equation:

$$F_d = \frac{.05\,(bC + F)}{.05\,V + (bC + F)} + F , \qquad (22)$$

where C is a constant dependent on the material and tooth error and F is the total applied or transmitted load. F_d should not exceed the static load strength of the tooth as based on the static stress of the material. Normally, Buckingham's equation for tooth wear, $F_w = D_1 b K Q$, must also be considered; however, since this mechanism was expected to operate for only a limited number of cycles, this requirement was neglected.

Restraining Cord

Several cord materials were tested in an effort to find the most suitable. Solid stainless-steel wire was discovered to be most unsatisfactory since the high resiliency of this wire tended to unwind the mechanism; braided copper wires were much more satisfactory, but the size required did not possess sufficient strength. Dacron and nylon cords were found to be best suited to this equipment. Test performed with same size cords showed that the dacron has a higher strength than nylon; but because nylon has the ability to stretch more readily, it was found to possess better shock-absorbing characteristics. A 96-lb test line of braided nylon was selected.

TESTING

To determine the adequacy of the design, both structurally and functionally, two component tests besides the systems environmental tests were utilized (Reference 5). The design passed the environmental tests without any major difficulty. One minor incident was encountered during the 600 cps resonance vibration test in the axial direction as the cords unwound from the pulley. The problem did not occur after the cord retaining springs were added (Figure 2). To determine the load capacity of the mechanism, a fixture with simulated booms was mounted (Figure 8). Dimensions A, B, and C were approximately the same as those on the actual spacecraft. The weights, equal to the maximum calculated centifugal force acting on the booms, were attached to the cg of each boom. Calculations indicated that centifugal force on the booms is maximum when $\theta = 35°$; therefore distance c was selected so that the cord from the weight would be normal to the boom when the booms are 35° from the vertical axis. The booms were held in place by wrapping a cord around them and were released by cutting the cord, thus simulating the loading condition at the time of boom release. This test revealed several design weaknesses, which have been corrected accordingly.

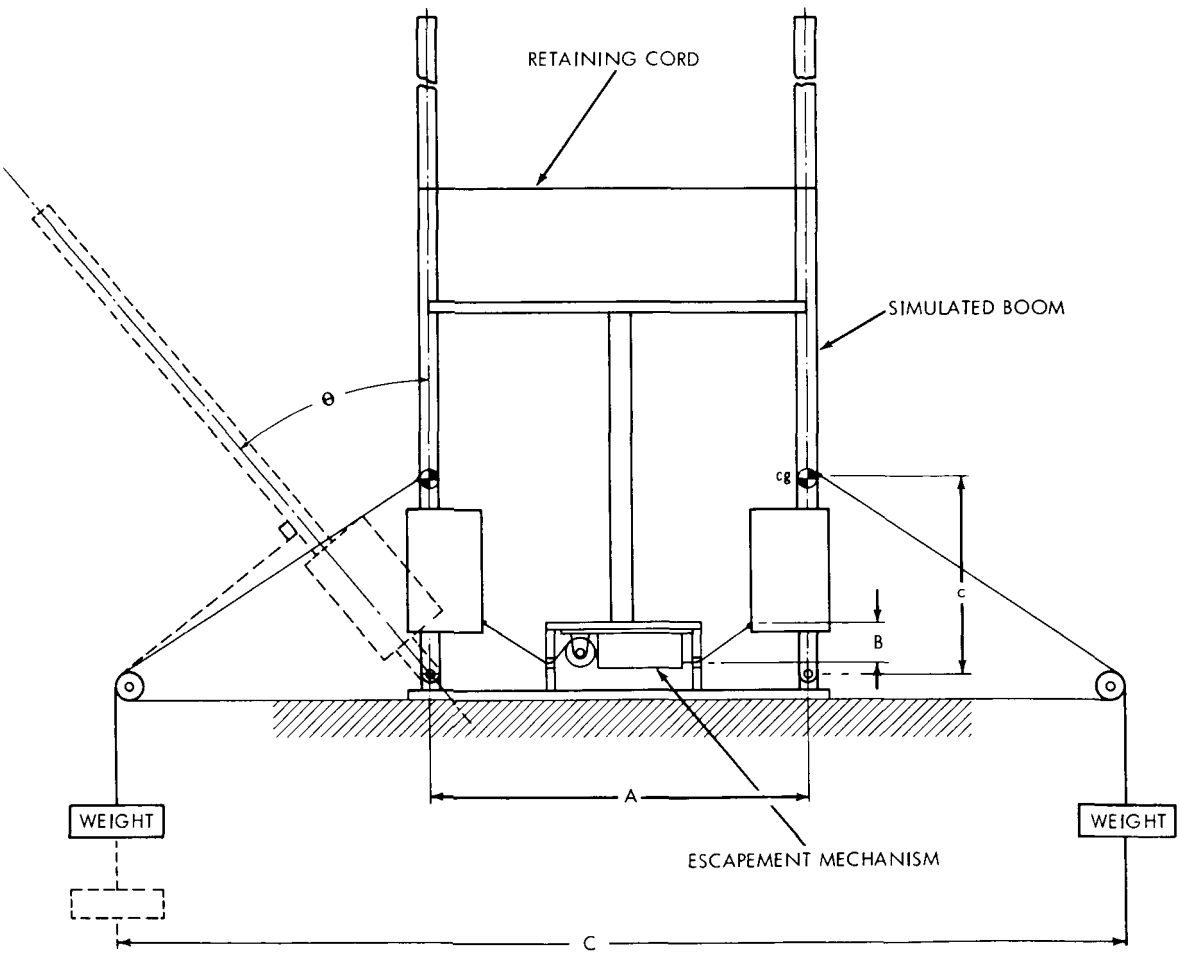

Figure 8—Component Test Set-up Simulating Initial Loading Condition on Escapement Mechanism.

The second component test was to determine whether the design functioned as intended. Figure 9 illustrates the test setup: The spacecraft structure (less the top dome) was mounted on the separation unit, which in turn was attached to the "dutchman." This configuration was then fastened to an empty X-248 bottle, and the system was inverted and mounted on a spin table with the roll moment of inertia properly simulated. The booms were held in position with scissor clamps (similar in design to proposed flight components); pressure was applied to the clamps through a wire wrapped around the legs of these clamps. The ends of this wire were locked in place by a pyrotechnic-actuated release mechanism. To measure the boom erection time, micro switches were placed at the folded and extended positions.

To simulate zero g, a constant force spring with a pull equal to approximately the weight of the boom was first tested by attaching one end of the spring to the cg and was later fastened to a point where equilibrium was achieved—between the weight of the boom and the pull of the spring—when the booms were very near the fully extended position. The booms were tested at 63, 74, and 90 rpm. Significant results were attained when the springs were attached to the boom's cg. Deployment time was within the expected range, and the booms locked in position each time. With the spring fastened to the second position described above, erection time remained approximately the same, but the booms were about 1/16 in. from lock-in position. Upon investigation to ascertain the reason for the difference in performance between the two systems, it was discovered that, with the spring attached to the cg, equilibrium condition could be obtained when the booms were between 15 and 75 degrees from the vertical axis. When the booms were at positions outside this range, however, the weights of the booms predominated and overcame the spring force. When the spring was fastened to the second position described, equilibrium could be attained only when the booms were between 60 and 90 degrees from the vertical axis. If the booms were lying in any position outside this range, the spring force prevailed and pulled the booms toward their folded positions (Figure 9). Neither system offered a satisfactory test inasmuch as the first was inclined to under-test and the second to over-test.

The constant spring force was found to vary as much as 3 pounds depending on the amount of unwinding. Also the inability to duplicate the spin's decay rate affected the test results to some extent. To increase the possibility for complete boom deployment, the boom hinge spring was made stronger so that the spring preload was approximately twice the torque needed to actuate the escapement mechanism. In the event that the centrifugal force near the end of boom travel may be too weak to overcome the inertia of the energy absorber, the spring would be able to assist in completing this task.

CONCLUDING REMARKS AND RECOMMENDATIONS

Ariel I was successfully launched in the spring of 1962. All boom-mounted instruments were reported working satisfactorily. However, according to Dr. Willmore,* a senior U.K. scientist on the project, "The erection of booms and paddles occurred prematurely about 1 to 2 minutes after injection." The appendages were deployed in four separate events as indicated by the satellite's decreasing

*A. P. Willmore, Private communication.

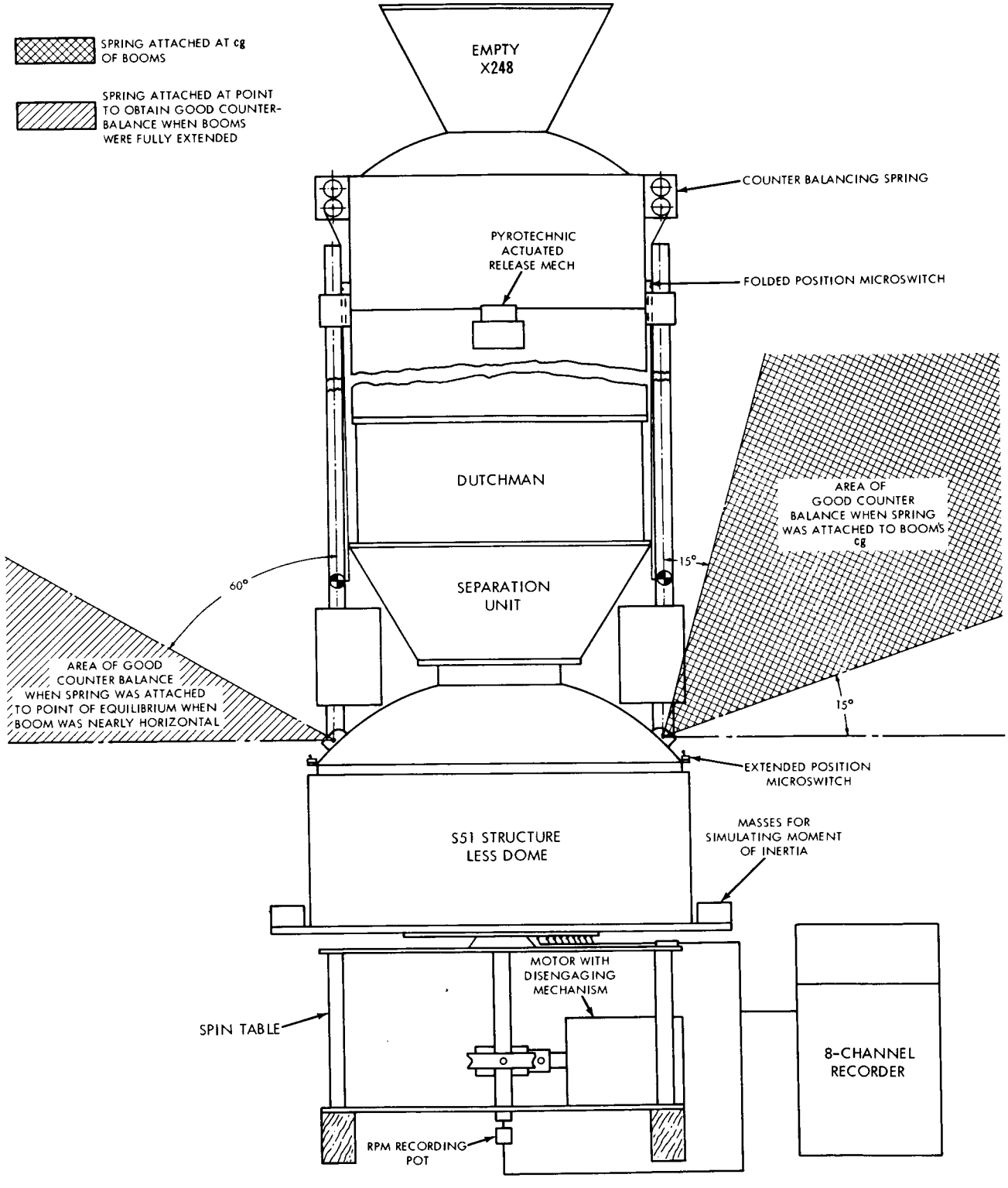

Figure 9—Test Set-up to Determine Whether Escapement Mechanism Met Design Requirement.

spin rate in "four well-defined steps." At the end of each of the first three de-spins "short duration shocks, such as might be caused by the booms snapping into place" were recorded from the accelerometers mounted orthogonally inside the dutchman. "For the fourth de-spin, where there is no shock, the duration of de-spin is slightly greater. The moment of inertia change corresponds with the erection of an experiment boom, so that this boom might have been successfully restrained by the escapement fitted for the purpose. Moreover, some 136-Mc telemetry was also received at Antigua. This shows a sudden and very marked change in the null of the electron density experiment at about this time, confirming that the boom erected here."

It may be also pointed out that the booms were so retained that any abnormal deployment could cause one boom to be released ahead of the other. Dr. Willmore's interpretation of the data indicated that the first boom—electron temperature—was released at a spin rate at least 10 rpm higher than the maximum design rate of 90. This situation probably caused the restraining cord to break. The electron density boom was released at approximately 90 rpm and was successfully restrained.

With due awareness of the circumstances and observations as quoted above, we are of the belief that this principle can be utilized advantageously in other similar applications. For future designs, it is suggested that a refined rewind mechanism be added to alleviate the rewinding problem. Addition of a locking mechanism that would cage the energy absorber in place during power flight and that could be released by the pull of the restraining cords might be beneficial. The energy absorber should be designed to control only the initial movement of the moving body and allow the body to complete its movement unrestrained by momentum. Such control would facilitate testing and increase the reliability of the design.

ACKNOWLEDGMENTS

The author is grateful to Messrs. J. Kauffman, A. Pierro, and J. Sween for their recommendations and untiring efforts in testing the final product.

REFERENCES

1. Fairman, S., and Cutshall, C. S., "Engineering Mechanics," 2nd Ed., New York: Wiley, 1946.
2. Steele, T. K., "Clock-Escapement Mechanisms," *Product Eng.* 28(1):179-185, January 1957.
3. Rawlings, A. L., "The Science of Clocks and Watches," 2nd Ed., New York: Pitman, 1948.
4. Norman, C. A., Ault, E. S., and Zarobsky, I. F., "Fundamentals of Machine Design," New York: Macmillan, 1938.
5. "Environmental Test Specifications for Design Qualification and Flight Acceptance Tests of The International Ionosphere Satellite—S-51," Goddard Space Flight Center, December 6, 1961.